Distribution of residence times in bistable noisy systems with time-delayed feedback

D. Curtin,[1] S. P. Hegarty,[1] D. Goulding,[1] J. Houlihan,[1] Th. Busch,[1] C. Masoller,[2] and G. Huyet[1]
[1]*Physics Department, National University of Ireland, University College, Cork, Ireland*
[2]*Instituto de Física, Facultad de Ciencias, Universidad de la República, Igua 4225, Montevideo 11400, Uruguay*
(Received 23 February 2004; published 10 September 2004)

We analyze theoretically and experimentally the residence time distribution of bistable systems in the presence of noise and time-delayed feedback. We explain various nonexponential features of the residence time distribution using a two-state model and obtain a quantitative agreement with an experiment based on a Schmitt trigger. The limitations of the two-state model are also analyzed theoretically and experimentally using a semiconductor laser with optoelectronic feedback.

DOI: 10.1103/PhysRevE.70.031103 PACS number(s): 05.40.Ca, 42.65.Pc

I. INTRODUCTION

Ever since Kramers' breakthrough results on thermally activated barrier crossings [1] the behavior of bistable dynamical systems in the presence of noise has attracted attention and found applications in many branches of science ranging from medicine to quantum optics [2]. Major achievements in the field include the discovery of stochastic [3,4] and coherence resonance [5], excitability, and noise induced synchronization [6,7]. However, most of these results apply to Markovian systems only and neglect possible effects of memory. Delay constitutes one of the simplest ways to incorporate memory into stochastic dynamical systems and it typically arises in feedback loops due to the finite velocity of propagation of information.

The case of stochastic bistable systems under the influence of time-delayed feedback was recently studied using a two-state model with transition rates dependent on the past state of the system [8]. This was an approximation of the time-delayed ordinary differential equation

$$\dot{x} = -\frac{\partial V(x)}{\partial x} + \epsilon x(t-\tau) + \sqrt{2D}\xi(t), \tag{1}$$

where $\xi(t)$ is a Gaussian white noise with $\langle \xi \rangle = 0$ and a δ-function correlation of strength D. This approximation was later used [9,10] to describe the distribution of residence times and analyze experimental measurements of the same. The aim of this paper is to analyze the effects of memory in further detail. Section II reviews the results of Refs. [8–10] and presents an experiment based on a Schmitt trigger (ST) with time-delayed feedback. As the ST is a good approximation to the two-state model, we demonstrate an excellent quantitative agreement with the predictions of the nonlinear model with feedback [8]. Section III highlights differences between the two-state model and continuous models described by a Langevin equation (1). In particular, we predict and show that effects at multiples of the delay time can be observed in the residence time distribution (RTD). We show that such behavior can be observed in an experiment [10] which consists of a vertical cavity surface emitting laser (VCSEL) with optoelectronic feedback.

II. THE TWO-STATE MODEL

A. Theory

In the remainder of this paper, we will consider Eq. (1) where the potential $V(x)$ is an even function with two minima at $\pm a$ separated by a local maximum at zero. A simple example of such a potential is the quartic potential $V(x) = x^4/4 - x^2/2$ with minima at ± 1. In this case, the Langevin equation (1) reads

$$\dot{x} = x - x^3 + \epsilon x(t-\tau) + \sqrt{2D}\xi(t). \tag{2}$$

Without delay ($\epsilon = 0$) this equation describes the behavior of an overdamped particle in the potential $V(x)$ and in the absence of noise the particle's dynamics becomes trivial once it has reached a stationary state. The presence of noise, however, will generate not only small fluctuations near these fixed points but also abrupt transitions between the two metastable states. The RTD for each well then follows Kramers' law $\rho(T) = r_K \exp[-r_K T]$, where the transition rate r_K is the so-called Kramers rate

$$r_K = \frac{\sqrt{V''(x_m)|V''(x_0)|}}{2\pi} \exp\left[-\frac{V(x_0) - V(x_m)}{D}\right],$$

where x_m and x_0 are the positions of the potential maximum and minimum, respectively. In the presence of memory, the exact analysis of Eq. (2) is complicated; however, it simplifies greatly if one assumes that $x(t)$ and $x(t-\tau)$ are independent variables and include the memory term in the potential, which then becomes a function of both x and $x_\tau = x(t-\tau)$:

$$U(x, x_\tau) = V(x) + \epsilon x_\tau x. \tag{3}$$

From this, one can see immediately that the potential barrier height depends on the sign of $x x_\tau$ and the escape rate therefore will depend on the value of x_τ. As a simple approximation that still captures the interesting dynamics for small values of ϵ, a two-state model describing a variable $s(t)$ which switches randomly between two values $s(t) = \pm 1$ was introduced in [8]. The feedback is incorporated by a time dependent switching rate

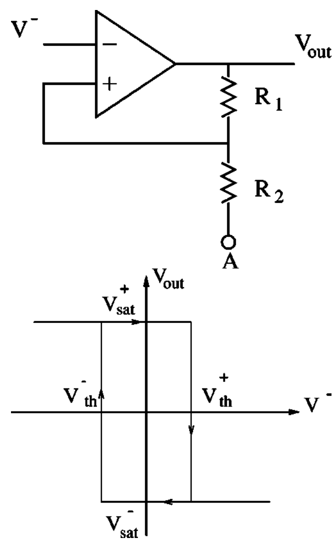

FIG. 1. Left: Circuit diagram of a Schmitt trigger. For a standard trigger, point A is grounded. For the modified circuit, the potential at A is proportional to the trigger output at a time τ previously. Right: Transfer function of a Schmitt trigger. The time taken by the trigger to transition from one saturation voltage to the opposite voltage takes several hundreds of nanoseconds. The typical residence time is of order 10 ms.

$$p(t) = \frac{p_1 + p_2}{2} + \frac{p_1 - p_2}{2} s(t)s(t-\tau), \tag{4}$$

which gives $p(t)=p_1$ if $s(t)=s(t-\tau)$ and $p(t)=p_2$ if $s(t)=-s(t-\tau)$. Using this model, it is possible to analytically calculate the power spectrum [8] and find piecewise analytical expressions for the escape rates' dependence on the residence time [9,10].

To understand the main features of the RTD, we can first consider that a switch from -1 to $+1$ occurs at $t=0$. Then $s(t-\tau)=-1$ for $t\to\tau^-$ and $p(t)=p_2$ in this limit. Similarly, if the particle remains in the state $s=+1$ for $t>\tau$, then $s(t-\tau)=+1$ and $p(t)=p_1$ for this time interval. The value of the switching rate for $t<\tau$ is not as obvious as the value of $s(t)$ is in general unknown for $t<0$. However, in the limit of large τ it can be shown that the switching rate is $p(t)=\sqrt{p_1p_2}$ for small residence time and deviates from this expression as t approaches $\tau-T_k$ [10], where $T_k=1/r_k$ is the Kramers switching time.

B. Experimental implementation using a Schmitt trigger

An electronic circuit that closely follows the two-state model was implemented using a Schmitt trigger driven by noise and electrical feedback as described in Fig. 1; based on the input voltage and the input history, the output voltage can switch between its positive and negative saturated voltages $V_{\mathrm{sat}}^{+(-)}$. The ST has been successfully employed in investigations of the related phenomenon of stochastic resonance [11,12]. The threshold voltages are given by

$$V_{\mathrm{th}}^{+(-)} = \frac{R_2}{R_1 + R_2} V_{\mathrm{sat}}^{+(-)}. \tag{5}$$

The output vs input graph for the ST is given on the right hand side of Fig. 1. Noise was applied to the ST input to induce random switching as in [11]. In addition we used delayed feedback to reinject the ST output and generate a non-Markovian stochastic system.

The operational amplifier used in this experiment was an LM301, a general purpose operational amplifier. The noise driving the input V^- of the trigger was generated from fluctuations in the breakdown voltage of a reverse biased Zener diode. This noise was amplified before it was low pass filtered to 50 kHz, chosen as it was much slower than the transition time of the trigger [13]. A power spectrum of the noise source was flat with a coherence time of 20 μs. The probability distribution function of the source showed it to be approximately Gaussian, with a root-mean-square voltage of $\sim$150 mV. The delay line was implemented using a digital acquisition board (National Instruments PCI-6040E) and a PC memory buffer. Delays of 10 ms and greater were used in this experiment.

The ST was first analyzed without any delayed electrical feedback. In this case, point A of Fig. 1(a) is held to ground and Eq. (5) holds, random switching was observed and the RTD was measured. The RTD follows an exponential decay, characteristic of Markovian stochastic systems. With constant noise voltage, the switching rate increased (decreased) as the threshold voltage was reduced (increased).

To implement the delayed electrical feedback V_{out} and point A of Fig. 1 were connected through the memory loop, the voltage at the point A was $\epsilon V_{\mathrm{out}}(t-\tau)$. With this circuit the two threshold voltages depended not only on $V_{\mathrm{sat}}^{+(-)}$ but also on $V_{\mathrm{out}}(t-\tau)$ as

$$V_{\mathrm{th}}^{+(-)}(t) = \frac{R_2 V_{\mathrm{sat}}^{+(-)} + \epsilon R_1 V_{\mathrm{out}}(t-\tau)}{R_1 + R_2}. \tag{6}$$

As in the model developed in Sec. II A, this system had two Kramers rates, depending on the value of $V_{\mathrm{out}}(t-\tau)$ which could be measured experimentally. This was easily done for this circuit by applying to point A of Fig. 1 a dc voltage corresponding to $\pm|\epsilon V_{\mathrm{sat}}^-|$ instead of the time-delayed output of the trigger.

The RTD of the system incorporating the memory loop is shown in Fig. 2 with the same feedback levels as used to measure p_1 and p_2. Data for both positive and negative values of ϵ are shown. From these we also calculated the ensemble average instantaneous switching rate $p(t)$ in order to compare with the theoretical predictions. As with the data obtained from numerical simulations of the two-state model, the RTD shows a discontinuity at the delay time τ. The probability distribution for short residence time is the same for both signs of ϵ as both have the same switching rate. From the measured values of p_1 and p_2, $\sqrt{p_1p_2}$ is calculated and found to match very well the measured switching rate for short residence times. For longer residence times approaching the delay time τ, the switching rate diverged from $\sqrt{p_1p_2}$ and approached p_2. At τ there was an abrupt change in $p(t)$ from p_2 to p_1. The switching rate remained constant for residence times bigger than the delay time.

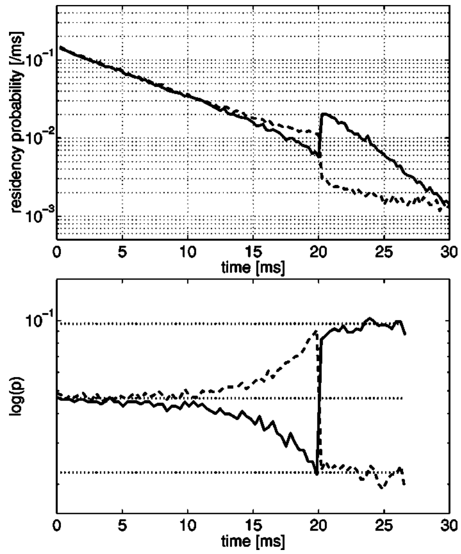

FIG. 2. Upper: Residence time distribution of the Schmitt trigger with both negative (solid line) and positive (dashed line) feedback. The feedback time is 20 ms. Lower: Transition rates as a function of time after transition for same data. Rates p_1 and p_2 are shown by dotted lines. The rate $\sqrt{p_1 p_2}$ is shown by a dotted line and is calculated from average values.

The ST therefore closely replicates the predictions of the two-state model. In the next section we will provide experimental results on a system that follows the continuous dynamics of (1) and demonstrate effects not captured by the two-state model.

III. CONTINUOUS BISTABLE DYNAMICAL SYSTEMS

A. Theory

Higher order features can be observed in the RTD of the continuous model described by Eq. (1). While the RTD of the two-state system for $T>\tau$ can be described by one constant transition rate, for the RTD of the continuous system an extra feature at 2τ can be observed [see Fig. 4(b) below]. This can be best understood by considering that the potential minima and barrier height shift, depending upon the state of the system a time τ previously. Consider the case where the particle is in the minimum $-a=-\sqrt{1+\epsilon}$ for $t<0$, a switch occurs at $t=0$ and the particle remains in the right-hand well for several τ. We define x_n as the location of the right-hand well minimum for $(n-1)\tau<t<n\tau$, i.e., x_n is defined by the sequence $x_n-x_n^3+\epsilon x_{n-1}=0$ for $n\geqslant 1$ with the initial condition $x_0=-a$. We therefore have a sequence of potentials separated in time by τ, $U_n(x)=U(x,x_{n-1})=x^4/4-x^2/2+\epsilon x_{n-1}x$, and as a result, a sequence of escape rates, as shown in Fig. 3. It is worthwhile to note that this calculation provides an explanation for the nonexponential decay of the RTD for $T>\tau$ but does not give the exact escape rate as the values of $x(t)$ prior to a jump are usually fluctuating.

Several papers have demonstrated that VCSELs undergoing random polarization switches allow experimental investigation of continuous bistable systems with noise. Experimental results on such systems with memory are presented in

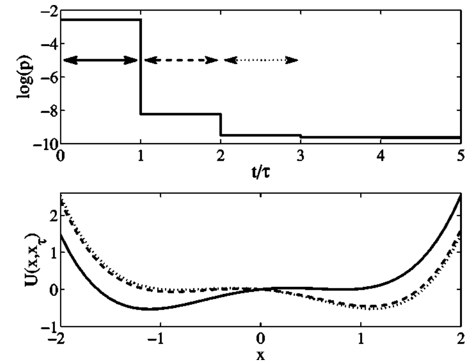

FIG. 3. Graphic illustrating the potentials and escape rates for the continuous system with a switch at $t=0$ and no switch for several τ subsequently. The major point to note is that the potential barrier height and the positions of the extrema change between $\tau<t<2\tau$ (dashed) and $2\tau<t<3\tau$ (dots), leading to different switching rates. Solid line is the potential barrier in the range $0<t<\tau$.

the following, where the features predicted above are clearly seen.

B. Experiment using the polarization dynamics of a VCSEL

To demonstrate the effects described in the subsection above, we analyze the behavior of a VCSEL with optoelectronic feedback as detailed in Ref. [10]. The output of these devices is usually linearly polarized but, as the injection current is increased, the emission may switch to the orthogonal polarization state. Around this switching point, a range of injection currents can be found where the laser's output spontaneously jumps between the two polarization states [14]. Previous experiments have shown that this switching rate follows Kramers' law in the case where spontaneous emission is sufficient to induce polarization switching [14] or if noise is added to the injection current [15]. This experimental arrangement has been used to reconstruct a potential [16].

As shown in the references above, the residence time in a VCSEL polarization state is a function of the injection cur-

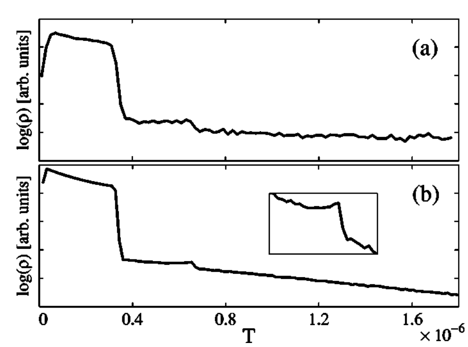

FIG. 4. (a) Experimental RTD of VCSEL system described in Sec. III B. A large discontinuity at $T=\tau$ can be seen as well as a smaller discontinuity at $T=2\tau$. (b) Simulations of continuous model of Eq. (2) showing discontinuities at $T=\tau$ and $T=2\tau$. Inset contains closeup of the discontinuity at $T=2\tau$. Here $D=0.07$.

rent. Using a polarization analyzer, a photodiode, and a delay line, we made the injection dependent upon the VCSEL polarization state at a time τ previously, and thus the escape rate from a polarization state was a function of the delayed state. Full experimental details can be found in Ref. [10] where it was shown that this experiment exhibits RTD similar to those obtained from numerical simulation of Eq. (2). However, for strong feedback levels the RTD distribution shows an increased switching rate at $T=2\tau$ as shown in Fig. 4 and explained in the previous section. Similar effects can be observed for negative feedback.

IV. CONCLUSIONS

We have presented experimental results on the residence time distributions of noisy time-delayed two-state dynamical systems. These experiments were based on a Schmitt trigger with a computer generated delay line, and the results are seen to be in quantitative agreement with previous theoretical predictions. We have also highlighted some limitations of using two-state models to analyze the behavior of delayed bistable systems described by a continuous variable. In particular, we demonstrated an enhancement or suppression of the switching rate at multiples of the delay time. This was illustrated by introducing a sequence of potentials to calculate the escape rate, and experimentally confirmed using a VCSEL with optoelectronic feedback where the switching rate enhancement was visible at twice the delay time. The experiment described above can be easily adapted to study more complicated systems such as those with colored noise or multiple memory loops.

ACKNOWLEDGMENTS

The authors acknowledge I. Kardosh, V. Voignier, and J. O'Callaghan at the Department of Optoelectronics, University of Ulm, Germany, for the VCSEL samples and R. Gillen and J. Sheehan for technical assistance. This work was supported by Science Foundation Ireland under Contract No. sfi/01/fi/co and by the TMR program of the Commission of the European Union through the VISTA network.

[1] H. Kramers, Physica (Utrecht) **7**, 284 (1940).
[2] P. Hänggi, P. Talkner, and M. Borkovec, Rev. Mod. Phys. **62**, 251 (1990).
[3] R. Benzi, A. Sutera, and A. Vulpani, J. Phys. A **14**, L453 (1981).
[4] L. Gammaitoni, P. Hänggi, P. Jung, and F. Marchesoni, Rev. Mod. Phys. **70**, 223 (1998).
[5] A.S. Pikovsky and J. Kurths, Phys. Rev. Lett. **78**, 775 (1997).
[6] B. Lindner, J. Garcia-Ojalvo, A. Neiman, and L. Schimansky-Geier, Phys. Rep. **392**, 321 (2004).
[7] C. Zhou and J. Kurths, Phys. Rev. Lett. **88**, 230602 (2002).
[8] L.S. Tsimring and A. Pikovsky, Phys. Rev. Lett. **87**, 250602 (2001).
[9] C. Masoller, Phys. Rev. Lett. **90**, 020601 (2003).
[10] J. Houlihan, D. Goulding, Th. Busch, C. Masoller, and G. Huyet, Phys. Rev. Lett. **92**, 050601 (2004).
[11] S. Fauve and F. Heslot, Phys. Lett. **97A**, 5 (1983).
[12] V.I. Melnikov, Phys. Rev. E **48**, 2481 (1993).
[13] L. Schimansky-Geier, J.A. Freund, A.B. Neiman, and B. Shulgin, Int. J. Bifurcation Chaos Appl. Sci. Eng. **8**, 869 (1998).
[14] M.B. Willemsen, M.U.F. Khalid, M.P. van Exter, and J.P. Woerdman, Phys. Rev. Lett. **82**, 4815 (1999).
[15] G. Giacomelli, F. Marin, and I. Rabbiosi, Phys. Rev. Lett. **82**, 675 (1999);S. Barbay, G. Giacomelli, and F. Marin, Phys. Rev. E **61**, 157 (2000).
[16] G. Giacomelli and F. Marin, Quantum Semiclassic. Opt. **10**, 469 (1998).